Amplitude death through a Hopf bifurcation in coupled electrochemical oscillators: Experiments and simulations

Yumei Zhai, István Z. Kiss, and John L. Hudson*
Department of Chemical Engineering, 102 Engineers' Way, University of Virginia, Charlottesville, Virginia 22904-4741, USA
(Received 9 September 2003; published 27 February 2004)

Amplitude death was observed in experiments with two coupled periodic electrochemical oscillators without time delay. Simulation results confirmed that the observed amplitude death was obtained via a Hopf bifurcation. The two oscillators must have a minimum discrepancy and both be near their individual Hopf bifurcations for amplitude death to occur. Phase drift (coexisting with unstable asymmetric phase-locked solutions), amplitude death, and in-phase synchronization were observed in both the experiments and simulations as coupling strength was increased. In addition, the simulations showed that a stable asymmetric phase-locked solution exists between the phase drift and amplitude death regions.

DOI: 10.1103/PhysRevE.69.026208 PACS number(s): 05.45.Xt, 82.40.Bj

I. INTRODUCTION

Coupled oscillatory systems have been intensively investigated in a variety of fields [1–3]. Examples include coupled solid-state lasers [4], oscillatory chemical reaction sites [5], yeast cells [6], and heart pacemakers [7,8]. The effect of coupling depends on both the coupling strength and the characteristics of the individual oscillators in the system. In weakly coupled systems the coupling is relatively weak compared with the attraction of the limit cycle. Phase models can describe the dynamical behavior when changes in the amplitudes can be ignored. Phase synchronization and emerging coherence [1,2,9,10] have been predicted by phase model studies and numerically and experimentally observed in weakly coupled physical, chemical, and biological systems [11,12]. In the case of strong coupling the effects on the amplitudes play an important role and produce behavior such as amplitude death [3,13–21] (AD) and dynamical clustering [22–24]. In amplitude death, oscillations cease due to strong coupling.

Amplitude death was detected in model studies of coupled chemical reaction [13,25–27]. More recent studies have shown that there are three different routes through which amplitude death can occur. In one route amplitude death is realized via a saddle-node bifurcation on the limit cycle when the oscillators are out-of-phase entrained with strong coupling [14]. The new stable steady states are thus created on or near the old limit cycle and are almost symmetric. AD has been observed with relaxation oscillators with the Belousov-Zhabotinsky reaction both numerically and experimentally in two or more coupled oscillators [14,28]. Another type of amplitude death comes from the lack of uniformity of the local frequency along the limit cycle of the coupled system; the coupling causes the system to slow down near some point and the frequency goes to zero [3]. This type of AD was shown to occur in a system of nondiffusively coupled neural oscillators. The third type of AD is obtained via a Hopf bifurcation among coupled oscillators with each near its Hopf bifurcation point. If the individual elements in the system are sufficiently different [15,29] or the coupling is time delayed [18,30], there is a range of intermediate coupling strengths within which the unstable focus of the system is stabilized by the coupling via a Hopf bifurcation. Experimental and model studies on a pair of time-delay coupled thermo-optical oscillators [19] and electronic circuit [20] exhibit this type of AD.

In this paper, we show amplitude death via a Hopf bifurcation in experiments without time delay in a coupled oscillatory chemical system. We used two electrochemical oscillators coupled through external electric circuit. Bifurcation diagrams of a model of two-coupled electrochemical oscillators were analyzed to confirm the experimental findings. Comparisons of our work with theoretical predictions of Aronson *et al.* [15] were made.

II. EXPERIMENT

A standard three-compartment electrochemical cell consisting of an array of two nickel working electrodes (1-mm diameter each with 2-mm spacing), a Hg-Hg_2SO_4-K_2SO_4 reference electrode (RE) and a Pt mesh counter electrode was used. A schematic of the experimental setup is shown in Fig. 1(a). The applied potentials V of the two electrodes were held at the same value with a potentiostat (EG&G Princeton

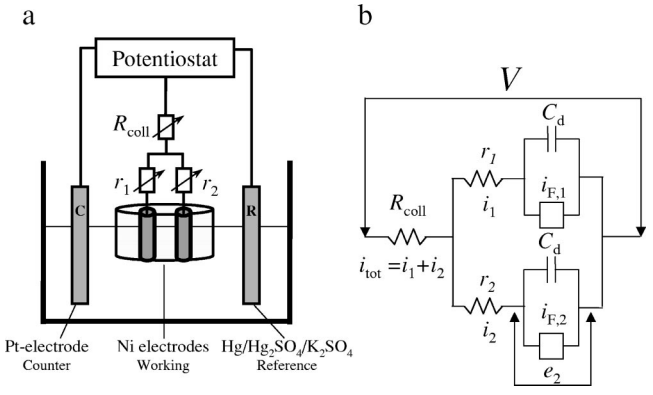

FIG. 1. Experimental apparatus (a) and equivalent circuit (b).

*Electronic address: hudson@virginia.edu

 ©2004 The American Physical Society

Applied Research, model 273). Experiments were carried out in 3 mol/dm^3 H_2SO_4 solution at a temperature of 11 °C. The solution was stirred with a magnetic stirrer at a speed of 250 rpm. The working electrodes are embedded in epoxy and the ends of the electrodes, where reaction takes place, are exposed to the electrolyte. The currents of the electrodes are measured independently at a sampling rate of 200 Hz.

The electrodes were connected to the potentiostat through two individual parallel resistors (r_k, $k=1,2$) and through one series collective resistor (R_{coll}) [see Fig. 1(a)]. Elektroflex EF-499 (Szeged, Hungary) computer controlled resistors were used to change the values of all the resistors during the experiments without opening the circuit. The collective resistor couples the electrodes and the ratio of collective to total resistance ε was used as a measure of the degree of coupling

$$\varepsilon = \frac{R_{\mathrm{coll}}}{R_{\mathrm{tot}}}, \tag{1}$$

where $R_{\mathrm{tot}}=R_{\mathrm{coll}}+r_1r_2/(r_1+r_2)$. For $\varepsilon=0$, the external resistance furnishes no additional coupling; for $\varepsilon=1$, maximal external coupling is achieved.

In experiments, the total external resistance remained a constant as $R_{\mathrm{tot}}=R_1R_2/(R_1+R_2)$, where R_1 and R_2 are equivalent individual resistance and their values are equal to $r_k(\varepsilon=0)$. The coupling ε was changed by varying the values of the collective resistance R_{coll} and the individual parallel resistances r_k according to $R_{\mathrm{coll}}=\varepsilon R_{\mathrm{tot}}$ and $r_k=(1-\varepsilon)R_k$, respectively. We employed this method to alter the coupling strength while holding all other parameters constant [31].

A simple equivalent circuit of two Ni electrodes in electrolyte is shown in Fig. 1(b). The electrical double layer at the metal-solution interface is described as a double layer capacitor C_{d} and a nonlinear Faradaic resistor in parallel. The current passing through the Faradaic resistor i_{F} is proportional to the rate of reaction of each electrode, which is determined by the reaction kinetics. The individual resistors r_k and collective resistor R_{coll} are inserted into the circuitry in parallel and in series, respectively. The individual current through each electrode i_k can be directly measured in experiments and thus serves as observable variable. However, the direct dynamical variable of this system, i.e., that which appears in the governing ordinary differential equation (ODE) model below, is the potential drop through the double layer e_k of the electrode. These two quantities are related by

$$i_k=(v-e_k)/r_k, \tag{2}$$

where r_k is the individual resistor of electrode k, v is the potential drop cross the individual resistor and the double layer [$v=V-R_{\mathrm{coll}}(i_1+i_2)$].

Figures 2(a) and 2(b) show polarization curves of two uncoupled Ni electrodes with the same external resistance of 400 Ω. The dynamics of these two individual electrodes are similar but not identical. Both of the current oscillations start and vanish through two supercritical Hopf bifurcations. In experiments, we used $R_{1,2}\approx 400$ Ω and studied amplitude death near the second Hopf bifurcation. Usually, even with the same external resistance, the exact values of the Hopf bifurcations are somewhat different because of heterogeneities caused by variations in the surface of the electrodes and transport. For instance, the second Hopf bifurcation occurs at $V=1.208$ V and $V=1.224$ V for electrode 1 and electrode 2 in Fig. 2, respectively. When the applied potential is within 10 mV cathodic to the second Hopf bifurcation (as indicated by the arrows in Fig. 2), the currents oscillate with a 3.5% difference in frequency. Large mismatch of the Hopf bifurcation points of the two electrodes can make the attractions to limit cycle of the two oscillations at a same potential (still within the oscillatory region) quite different. This is unfavorable for amplitude death because a relatively weak attraction to the limit cycle is required for both of the oscillators. Therefore, different external resistors for the two electrodes were used when necessary to make the two Hopf bifurcation points close to each other.

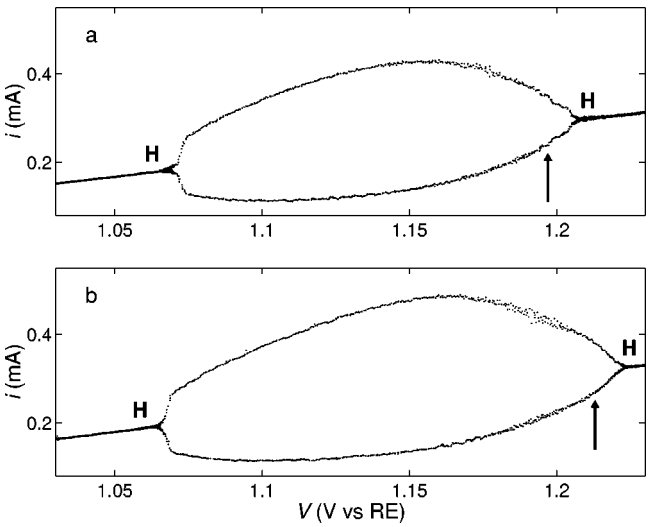

FIG. 2. Experiments: anodic polarization curves of two individual Ni electrodes in sulfuric acid. (a) Electrode 1. (b) Electrode 2. $R_1=R_2=400$ Ω, scan rate $=0.2$ mV/s. H represents the Hopf bifurcation. For periodic currents, only maxima and minima are shown. The arrows show where the applied potential V is 10 mV cathodic to the second Hopf bifurcation point.

The applied potential was held constant at 5–10 mV below the second Hopf bifurcation point. There was a slow drift of the Hopf bifurcation in the experiments toward higher potentials (about 1 mV every 3 min, and a typical experiment lasted for about 3 min). However, this drift does not weaken our conclusion of experimental amplitude death by coupling because it only slowly enhances the oscillatory state of the individual system.

III. RESULTS

A. Experimental results

The results of an experiment showing amplitude death of two coupled electrochemical oscillators are presented in Fig. 3. In this experiment, the equivalent individual resistances for the two electrodes were adjusted carefully to make the

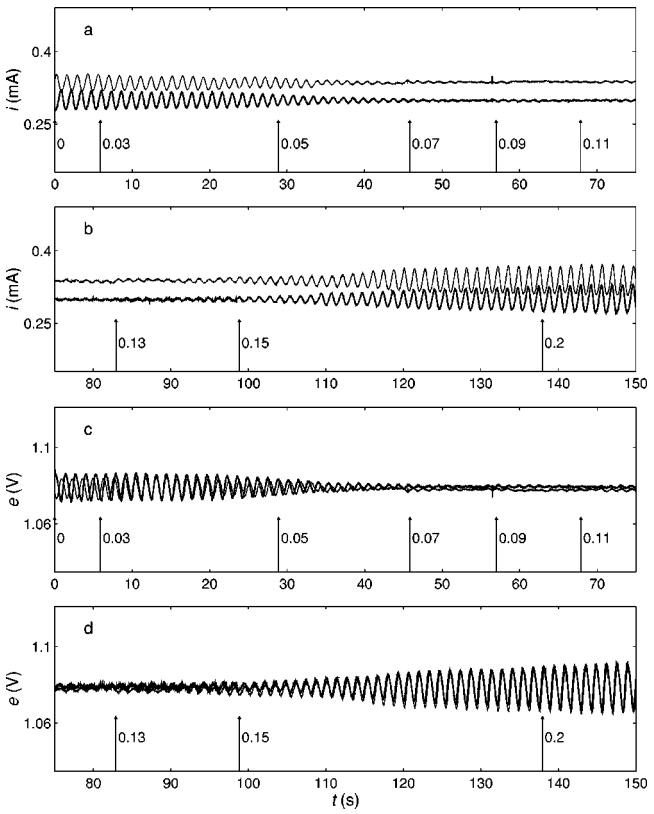

FIG. 3. Experiments: amplitude death and synchronization of two coupled oscillators. (a), (b) current (*i*) time series of two electrodes. Thin curve: electrode 1, $R_1 = 378\ \Omega$. Thick curve: electrode 2, $R_2 = 420\ \Omega$. The arrows show the points where the coupling strength ε was imposed. The number near each arrow is the value of ε. (c), (d) Time series of potential drops through the double layer (*e*) calculated from the currents in (a)–(b).

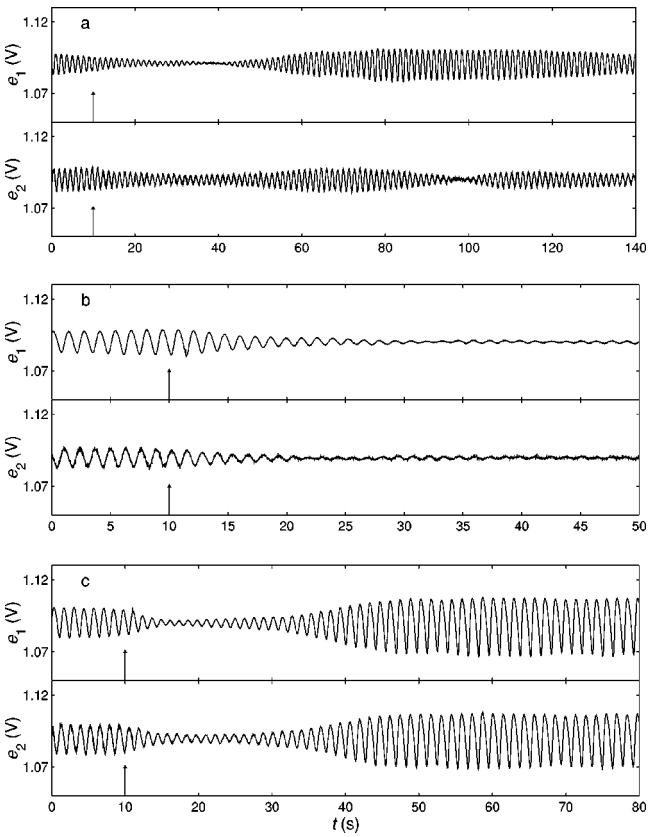

FIG. 4. Experiments: effects of coupling strengths. (a) $\varepsilon = 0.03$, quasiperiodic oscillations (phase drift). (b) $\varepsilon = 0.05$, amplitude death. (c) $\varepsilon = 0.15$, in-phase synchronized oscillations. Upper curve: electrode 1, $R_1 = 378\ \Omega$. Lower curve: electrode 2, $R_2 = 420\ \Omega$. The arrows show the points where the coupling was turned on.

Hopf bifurcation points close to each other; the difference was 2 mV. The currents of the two Ni electrodes were intrinsically oscillating without coupling, as shown in Fig. 3(a) during the first 6 s. There were differences of 3% in frequency and 12% in amplitude between the two individual oscillations. As the coupling strength was increased to $\varepsilon = 0.05$, amplitude death was observed for both oscillators. The system remained in a stable steady state until the coupling parameter was increased to 0.13, above which it developed into the synchronized oscillatory state as shown in panel (b) of Fig. 3. Thus amplitude death occurred in the region of the coupling parameter, $0.050 \leqslant \varepsilon \leqslant 0.13$. Note that the amplitudes of the synchronized oscillations were larger due to the slow drift.

The direct dynamical variable of this system, the potential drop through the double layer e_k, can be obtained from the measured current with Eq. (2). It is seen [in Figs. 3(c–d)] that the time series of the potentials e_k are very similar to those of the currents. The difference of the mean potentials is smaller than that of the mean currents. Further experimental results are only presented in terms of potential.

To examine the effects of coupling on the behavior of the system, longer time series at a specified coupling parameter were obtained. In Fig. 4(a) we see that at a very weak coupling strength both electrodes exhibited quasiperiodic oscillations on large time scales; this is called a phase drift solution [15]. At an intermediate coupling strength of 0.05, amplitude death occurred after some transient time (about 10 oscillations), as shown in Fig. 4(b). The transient to the steady state was through antiphase damped oscillations. (The coupling was imposed to the system at the moment at which the two oscillations were approximately antiphase; this effectively shortened the transient time.) Note that the steady states still had very small fluctuations; these fluctuations were often seen in experiments and likely caused by some inevitable experimental noise. (Noise has been shown to weaken the oscillator death in coupled limit cycle system [32].) A stronger coupling of $\varepsilon = 0.15$ resulted in a synchronized state [Fig. 4(c)]. Again, due to the drift in experiments, the synchronized oscillation had larger amplitude compared with the intrinsic oscillations without coupling.

When the Hopf bifurcation points of the two electrodes were somewhat wider separated, the two oscillators had greater differences in amplitude at the same applied potential *V* near the Hopf bifurcation. Amplitude death also occurred under such conditions as shown in Fig. 5. With the same equivalent individual resistance for the two electrodes, the intrinsic oscillations had a 66% difference in amplitude

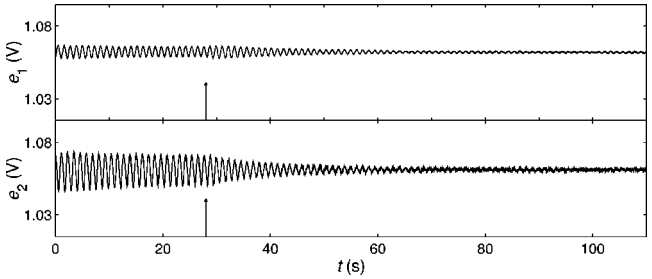

FIG. 5. Experiments: amplitude death for two oscillators with greater difference in amplitude. $R_1=R_2=400\ \Omega$. The arrow shows where $\varepsilon=0.05$ was applied.

(while the frequency difference was 2%). Stable steady states were observed at an intermediate coupling strength of $\varepsilon=0.05$.

B. Simulations

Model. Simulations on two coupled electrochemical oscillators were carried out to confirm the experimental findings and to explore the mechanism of amplitude death from bifurcation diagrams.

We used a model of anodic electrodissolution of a single nickel electrode proposed by Haim *et al.* [33]. The model in a dimensionless form involves two variables: the dimensionless double layer potential drop e and the surface coverage of NiO+NiOH (θ). Based on this kinetic model of a single electrode, the following dimensionless equations were derived for two coupled nickel electrodes:

$$\frac{de_k}{dt}=\frac{V-e_k}{R_k}-i_{\mathrm{F},k}(\theta_k,e_k)+\frac{2}{R_1+R_2}\frac{\varepsilon}{1-\varepsilon}(e_{\mathrm{mean}}-e_k), \tag{3}$$

$$\Gamma_k\frac{d\theta_k}{dt}=\frac{\exp(0.5e_k)}{1+C_{\mathrm{h}}\exp(e_k)}(1-\theta_k)-\frac{bC_{\mathrm{h}}\exp(2e_k)}{cC_{\mathrm{h}}+\exp(e_k)}\theta_k \tag{4}$$

where the subscripts $k=1,2$, identify the electrodes; V is the dimensionless applied potential; R_k is the dimensionless equivalent individual resistance; Γ_k is the surface capacity; and $i_{\mathrm{F},k}$ is the Faradaic current

$$i_{\mathrm{F},k}(\theta_k,e_k)=\left(\frac{C_{\mathrm{h}}\exp(0.5e_k)}{1+C_{\mathrm{h}}\exp(e_k)}+a\ \exp(e_k)\right)(1-\theta_k), \tag{5}$$

$e_{\mathrm{mean}}=(e_1+e_2)/2$ is the mean potential drop through the double layer. ε is the same coupling parameter as that in experiments.

Equation (3) is for the charge balance in the equivalent circuit [see Fig. 1(b)] of the electrochemical reaction; Eq. (4) is obtained from the simplified mass balance and kinetics. Since the coupling is electrical (through resistors), it only appears in the equation for the variable e. $\varepsilon=0$ represents uncoupled oscillators; $\varepsilon\to 1$ yields maximum global coupling that can completely synchronize the two oscillators.

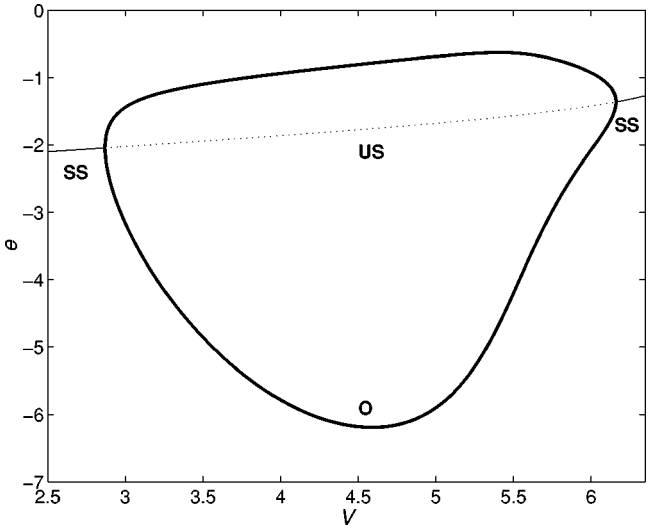

FIG. 6. Simulations: $e-V$ bifurcation diagram of a single electrode. $R=4.993$, $\Gamma=0.010\,05$. SS: stable steady state. US: unstable steady state. O: stable oscillatory solution, for which only maxima and minima of oscillations are shown.

The parameter values $C_{\mathrm{h}}=1600$, $a=0.3$, $b=6\times10^{-5}$, and $c=1\times10^{-3}$ were used [33] to obtain dynamical features similar to experiments. R_k's and Γ_k's were taken slightly different values for each electrode to simulate the heterogeneity. (Other choices also possible, however, these parameters seem to be the most reasonable ones.) We employed XPP bifurcation and continuation package for numerical analysis.

Results. Figure 6 shows a one-parameter (V) bifurcation diagram of a single electrode with $R_1=4.993$ and $\Gamma_1=0.010\,05$. It resembles the experimental bifurcation diagram (Fig. 2). The potential drop through the double layer (e) oscillates within the region set by two supercritical Hopf bifurcations. The second Hopf bifurcation occurs at $V=6.1508$. For another electrode with parameters $R_2=5.005$ and $\Gamma_2=0.009\,95$, the one-parameter bifurcation diagram is very similar to this one except that its second Hopf bifurcation point is slightly larger ($V=6.1513$). The oscillations at the second Hopf bifurcation points for electrode 1 and 2 have a difference in frequency of about 1%.

The results of a two-parameter (V-ε) bifurcation analysis of these two coupled oscillators are presented in Fig. 7. The inset of the enlargement of the lower coupling region shows that on crossing each Hopf bifurcation line the number of eigenvalues of the steady state with positive real parts is decreased by 2 and eventually becomes 0. On the vertical line of $\varepsilon=0$, when V is below H1 and H2, both the single electrodes are in oscillatory states. As some weak coupling is added, the system goes into the relatively narrow region with 4 positive eigenvalues of the steady state where the system has two unsynchronized oscillations, viz., the phase-drift solution. Stronger coupling moves the system into the region with 2 positive eigenvalues where phase-locked oscillations are observed. The ''V''-shaped locus of Hopf bifurcation outlines the region with no eigenvalues with positive real parts where the system is in a stable steady state. It is seen

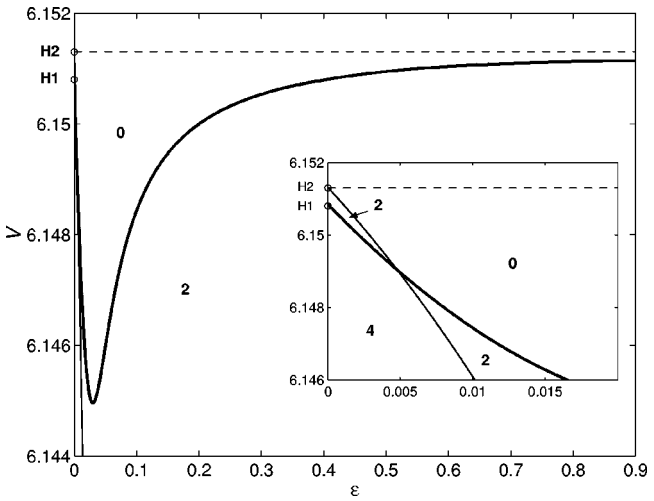

FIG. 7. Simulations: locus of Hopf bifurcation in V-ε parameter space. The two electrodes have the parameters of $R_1=4.993$, $\Gamma_1=0.010\,05$ and $R_2=5.005$, $\Gamma_2=0.009\,95$. Bold curve: Hopf bifurcation associated with electrode 1. Thin curve: Hopf bifurcation associated with electrode 2. H1, H2: Hopf bifurcation points of uncoupled electrode 1 and electrode 2, respectively. The numbers indicate the number of eigenvalues with positive real parts for the steady state in each region. Inset: enlargement of the region at very low coupling strength.

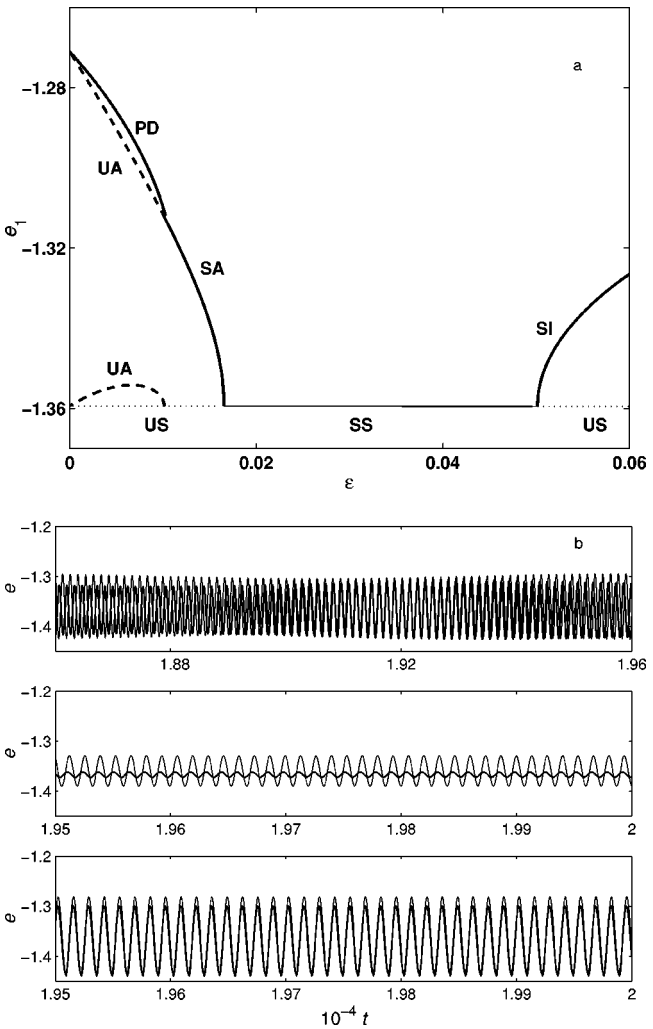

FIG. 8. Simulations: (a) Bifurcation diagram in ε-max e_1 space at $V=6.146$. The two electrodes have the same parameters as in Fig. 7. US: unstable steady state. SS: stable steady state (amplitude death). UA: unstable asymmetric oscillation. SA: stable asymmetric phase-locked oscillation. SI: stable in-phase oscillation. PD: phase-drift solution (quasiperiodic oscillation). (b) Time series of the potential (e) in three oscillatory regions of panel a. Top: $\varepsilon=0.0073$, phase-drift (PD) solution. Middle: $\varepsilon=0.013\,76$, stable asymmetric phase-locked oscillation (SA). Bottom: $\varepsilon=0.15$, stable in-phase oscillation (SI). Thick line: electrode 1. Thin line: electrode 2.

that amplitude death only occurs when the applied potential V is set near the Hopf bifurcation point around 6.151; this is, consistent with the results in experiments. As V decreases further away from H2, the ε region for amplitude death becomes narrower; below 6.1445, the stable steady state no longer exists in the whole range of coupling strength.

Figure 8(a) shows a detailed bifurcation diagram at $V=6.146$, in which the maximum of e_1 is shown as a function of ε. When there is no coupling, the system consists of two independent, inherently slightly different oscillators. As the two oscillators are weakly coupled with $\varepsilon<0.010\,19$, the unstable steady state has 4 positive eigenvalues. Simultaneously, unstable asymmetric (UA) phase-locked oscillatory solutions are obtained. There are two of the UA because of the symmetry of the system. The stable state in this ε region is a torus in four-dimensional state space; thus a quasiperiodic oscillation or phase drift solution is observed for each subsystem [Fig. 8(b) top]. As the coupling strength is further increased, the torus is destroyed through a torus bifurcation at $\varepsilon=0.010\,19$ and one stable asymmetric phase-locked solution appears. From Fig. 8(b) (middle) we see that the two elements oscillate with the same frequency while there remains a relatively large difference in their amplitudes. The amplitudes of both oscillators in this synchronized state decrease with coupling until a Hopf bifurcation occurs at $\varepsilon=0.016\,55$. Amplitude death occurs within $0.016\,55<\varepsilon<0.050\,14$, corresponding to the region of 0 eigenvalues with positive real parts in Fig. 7 at this applied potential. Above the Hopf bifurcation at $\varepsilon=0.050\,14$, the system oscillates in synchrony again. This later synchronized state is different from that seen before amplitude death. As seen from the time series at $\varepsilon=0.15$ [Fig. 8(b) bottom] the system now exhibits in-phase synchronization with similar amplitudes. The two synchronized states, before and after the amplitude death, correspond to the region with 2 positive eigenvalues of Fig. 7.

In experiments the two oscillators are inherently different because of heterogeneity and because of the different individual resistors. In simulations, we model the nonidentical nature of the oscillators by using different values for the parameters R and Γ. To investigate the effect of heterogeneity on amplitude death, a heterogeneity parameter ΔH was used to change both R and Γ for the two oscillators simultaneously as $R_{1,2}=R_0\pm\Delta H\times\Delta R$, $\Gamma_{1,2}=\Gamma_0\pm\Delta H\times\Delta\Gamma$, where $R_0=4.999$, $\Delta R=6\times10^{-3}$, $\Gamma_0=0.01$, $\Delta\Gamma=5\times10^{-5}$. $\Delta H=1$ is the case for which results have been shown in Figs. 6–8. When $\Delta H=0$, the two oscillators are

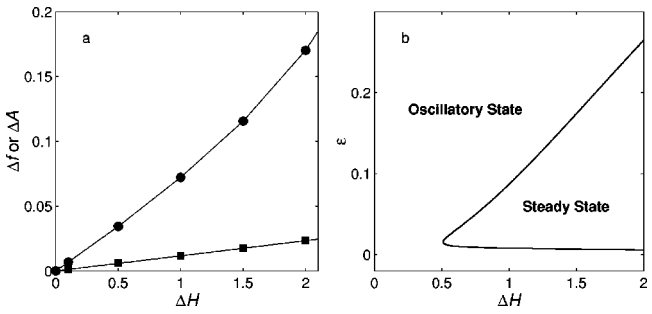

FIG. 9. Simulations: (a) Effect of heterogeneity parameter ΔH on oscillations (with fixed $V=6.148$). Square: Δf, the relative difference in frequency. Circle: ΔA, the relative difference in amplitude. (b) Locus of Hopf bifurcation in ΔH-ε parameter space.

identical. The greater ΔH, the greater difference both in frequency and in amplitude as shown in Fig. 9(a). From the bifurcation diagram in ΔH-ε space [Fig. 9(b)], we see that amplitude death occurs within a "<"-shape locus of Hopf bifurcations at $V=6.148$. The limit of the amplitude death region on the left part of the diagram indicates a minimum difference of the two oscillators for amplitude death. At different applied potentials, the two-parameter bifurcation diagram in ΔH-ε space are similar to the one shown here but the minimum ΔH for amplitude death is larger when the applied potential is smaller than 6.148. Two factors might contribute to this: the attraction to limit cycle is stronger when the applied potential is lower and thus conditions for amplitude death are less favorable. Also, the frequencies and amplitudes of the two oscillators are more similar at applied potentials further away from their Hopf bifurcation points and thus a greater value of ΔH is required for amplitude death.

IV. DISCUSSION

Amplitude death was experimentally observed with two coupled periodic electrochemical oscillators without time delay. Simulation results confirm that the observed amplitude death is obtained via a Hopf bifurcation. The coupling shifts the supercritical Hopf bifurcation of the whole system with respect to those of the individual oscillators so that a stable steady state is obtained at applied potentials lower than the individual Hopf bifurcation points. The two oscillators must have a minimum discrepancy and both be near their individual Hopf bifurcations for amplitude death to occur. Herrero *et al.* [19] and Reddy *et al.* [20] studied similar type of amplitude death experimentally with a pair of thermo-optical oscillators and a pair of nonlinear electronic circuits, respectively, but these systems are coupled with time delay. Herrero *et al.* pointed out that the transient to the stable steady state was through antiphase damped oscillations in their experiments. This is also true in our chemical system.

As expected from the results of a theoretical study on this type of amplitude death [15], phase drift (coexisting with unstable asymmetric phase-locked solutions), amplitude death, and in-phase synchronization were observed both in experiments and in simulations as the coupling strength was increased. However, an "additional state," the stable asymmetric phase-locked solution, exists between phase drift and amplitude death regions in our simulations. This shows that the asymmetric phase-locked solution which is always unstable in a simplified system with identical oscillator amplitudes studied by Aronson *et al.* [15] can become stable in real coupled systems. In the electrochemical system studied here, as in experiments in general, the individual oscillators have somewhat different amplitudes as well as frequencies and the system is influenced by inherent noise and slow drift.

Nevertheless, the amplitude death via a Hopf bifurcation discussed analytically by Aronson *et al.* [15] does exist in an electrochemical oscillatory system. The coupled electrochemical oscillators provide a model experimental system for the study of amplitude death without time delay.

ACKNOWLEDGMENTS

This work was supported by the National Science Foundation (Grant No. CTS-0000483) and the Office of Naval Research (Grant No. N00014-01-1-0603).

[1] Y. Kuramoto, *Chemical Oscillations, Waves and Turbulence* (Springer, Berlin, 1984).
[2] A.T. Winfree, *The Geometry of Biological Time* (Springer-Verlag, New York, 1980).
[3] G.B. Ermentrout and N. Kopell, SIAM (Soc. Ind. Appl. Math.) J. Appl. Math. **50**, 125 (1990).
[4] R.A. Oliva and S.H. Strogatz, Int. J. Bifurcation Chaos Appl. Sci. Eng. **11**, 2359 (2001).
[5] G. Ertl, Science **254**, 1750 (1991).
[6] A.K. Ghosh, B. Chance, and E.K. Pye, Arch. Biochem. Biophys. **145**, 319 (1971).
[7] A.T. Winfree, J. Theor. Biol. **16**, 15 (1967).
[8] D.C. Michaels, E.P. Matyas, and J. Jalife, Circ. Res. **61**, 704 (1987).
[9] H. Daido, Physica D **91**, 24 (1996).
[10] S.H. Strogatz, Physica D **143**, 1 (2000).
[11] A.S. Pikovksy, M.G. Rosenblum, and J. Kurths, *Synchronization: A Universal Concept in Nonlinear Science* (Univeristy Press, Cambridge, 2001).
[12] I.Z. Kiss, Y.M. Zhai, and J.L. Hudson, Science **296**, 1676 (2002).
[13] K. Bar-Eli, Physica D **14**, 242 (1985).
[14] M.F. Crowley and I.R. Epstein, J. Phys. Chem. **93**, 2496 (1989).
[15] D.G. Aronson, G.B. Ermentrout, and N. Kopell, Physica D **41**, 403 (1990).
[16] M. Dolnik and I.R. Epstein, Phys. Rev. E **54**, 3361 (1996).
[17] A. Stefanski and T. Kapitaniak, Phys. Lett. A **210**, 279 (1996).
[18] D.V.R. Reddy, A. Sen, and G.L. Johnston, Phys. Rev. Lett. **80**, 5109 (1998).
[19] R. Herrero, M. Figueras, J. Rius, F. Pi, and G. Orriols, Phys. Rev. Lett. **84**, 5312 (2000).

[20] D.V.R. Reddy, A. Sen, and G.L. Johnston, Phys. Rev. Lett. **85**, 3381 (2000).
[21] L.L. Rubchinsky, M.M. Sushchik, and G.V. Osipov, Math. Comput. Simul. **58**, 443 (2002).
[22] K. Kaneko, Phys. Rev. Lett. **63**, 219 (1989).
[23] D.H. Zanette and A.S. Mikhailov, Phys. Rev. E **62**, R7571 (2000).
[24] W. Wang, I.Z. Kiss, and J.L. Hudson, Chaos **10**, 248 (2000).
[25] K. Bar-Eli, J. Phys. Chem. **88**, 6174 (1984).
[26] K. Bar-Eli and S. Reuveni, J. Phys. Chem. **89**, 1329 (1985).
[27] K. Bar-Eli, J. Phys. Chem. **88**, 3616 (1984).
[28] M. Yoshimoto, Chem. Phys. Lett. **280**, 539 (1997).
[29] G.B. Ermentrout, Physica D **41**, 219 (1990).
[30] D.V.R. Reddy, A. Sen, and G.L. Johnston, Physica D **129**, 15 (1999).
[31] I.Z. Kiss, W. Wang, and J.L. Hudson, J. Phys. Chem. B **103**, 11 433 (1999).
[32] L. Rubchinsky and M. Sushchik, Phys. Rev. E **62**, 6440 (2000).
[33] D. Haim, O. Lev, L.M. Pismen, and M. Sheintuch, J. Phys. Chem. **96**, 2676 (1992).